

## 59.1: Invited Paper: Optoelectronic OLED Modeling for Device Optimization and Analysis

**Beat Ruhstaller, Thomas Flatz, Michael Moos, and Guido Sartoris**

Center for Computational Physics, Zurich University of Applied Sciences, Winterthur, Switzerland

**Michael Kiy, Tilman Beierlein, Roland Kern, and Carsten Winnewisser**

Polymer Optoelectronics Division, Centre Suisse d'Electronique et de Microtechnique, Zurich, Switzerland

**Roger Pretot, Natalia Chebotareva, and Paul van der Schaaf**

Group Research, Ciba Specialty Chemicals Inc., Basel, Switzerland

### 1. Introduction

Organic light-emitting devices (OLEDs) consist of a stack of multiple thin film layers whose thicknesses influence both the optical and electronic performance. Upon injection and transport, the charge carriers may recombine to form excitons that diffuse and decay radiatively, thus leading to distinct recombination and emission zone profiles that determine device performance. Suitable simulation tools that allow a better understanding and efficient optimization of organic optoelectronics devices and materials are desirable.

### 2. Device Model

Numerical simulations have been used in the past to describe the electronic [1,2] and the optical processes [3,4,5] in multi-layer OLEDs.

#### 2.1. Electronic Model

The key ingredients of our device model were outlined in reference [1] and are reproduced below for clarity:

$$\frac{\partial E(x)}{\partial x} = \frac{e}{\epsilon \epsilon_0} (p(x) - n(x)) \quad (1)$$

$$J_e(x) = e \mu_e(x, E) \cdot n(x) \cdot E(x) + D(\mu) \cdot \frac{\partial n(x)}{\partial x} \quad (2)$$

$$\frac{\partial n(x)}{\partial t} = \frac{1}{e} \frac{\partial J_e(x)}{\partial x} - r(x) \cdot p(x) \cdot n(x). \quad (3)$$

Here,  $n$  is the density of electrons,  $p$  the density of holes,  $E$  the electric field and  $r = (e / \epsilon \epsilon_0) \cdot (\mu_e + \mu_h)$  the Langevin recombination rate coefficient. The field dependent mobility is assumed to follow the universal Poole-Frenkel form

$$\mu(E) = \mu_0 \exp(\sqrt{E/E_0}) \quad (4)$$

where  $\mu_0$  is the zero field mobility and  $E_0$  the characteristic field. The rate equation for singlet excitons contains a generation, a diffusion and a radiative decay term

$$\frac{\partial S(x)}{\partial t} = \gamma \cdot r(x) \cdot n(x) \cdot p(x) + D_S \cdot \frac{\partial^2 S(x)}{\partial x^2} - \frac{S(x)}{\tau} \quad (5)$$

The prefactor  $\gamma$  for the singlet exciton generation rate is typically taken to be 1/4 following the traditional spin statistics argument. Triplet excitons and guest molecule excitons can be treated analogous. We use the diffusion constant  $D_S = l^2 / \tau$ , with  $l$  being the diffusion length and  $\tau$  the exciton lifetime. Charge injection is assumed to be thermionic and affected by image charge recombination.

In this paper we present some simulation results from the electronic drift-diffusion model and demonstrate the combined electronic-optical simulation software called S-ETFOS, which is an extension of the emissive thin film optics simulator ETFOS [6]. The screenshot of S-ETFOS in Figure 1 shows the charge density profiles of an example bilayer OLED.

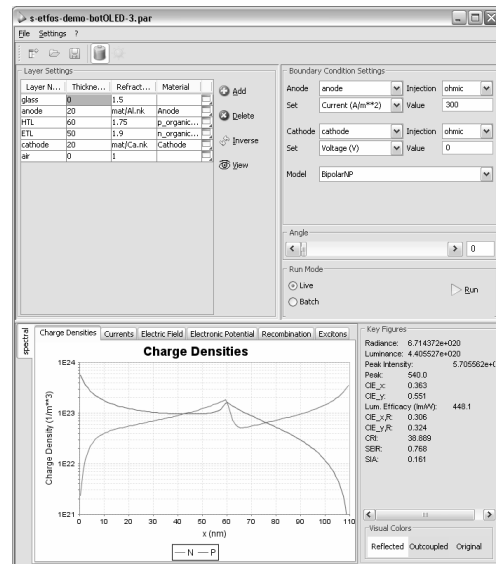


**Figure 1** Resulting charge density profile of a bilayer OLED calculated with the optoelectronic simulator S-ETFOS .

Device models for the electronic and excitonic processes in OLEDs are solved by suitable numerical methods. Advanced optimization and fitting algorithms need to solve the electronic device model equations repeatedly, thus relying on fast and stable solvers. In contrast to the optical OLED device simulations, the electronic device simulations have not yet achieved predictive

power. Therefore, they must be applied to experimental OLED data in a descriptive manner. Electronic device simulation often deals with the study of the impact that physical models or parameters have on the device performance.

For illustration purposes we consider the three distinct charge mobility models: a) constant mobility  $\mu_e = const$ , b) field-dependent mobility  $\mu_e = f(E)$  and c) density-dependent mobility  $\mu_e = f(n)$ , as previously compared by Blom et al. The simulation results with S-ETFOS for this comparison are shown in Figure 2 for single layer, electron-only devices and exhibit variations in the field profile depending on the mobility model used. Further details regarding the comprehensive electronic-optical OLED model will be discussed and published elsewhere.

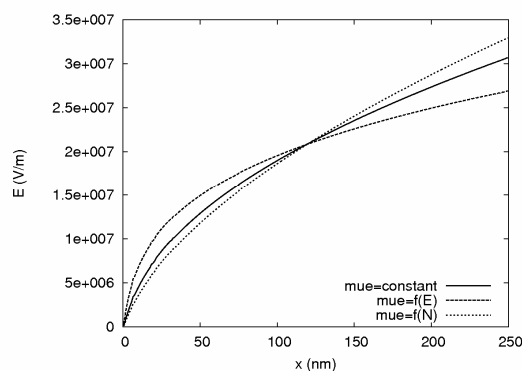


**Figure 2** Electric field profiles in single layer device with three different charge mobility models.

## 2.2. Optical Model

The emissive thin film optics simulator ETFOS [7], see Figure 1, considers the emission to originate from oscillating and thus radiative dipoles embedded in a multilayer thin film stack. The outcoupled emission spectra are calculated as a function of the viewing angle, polarisation and dipole orientation. The simulator allows the variation of wavelength, external viewing or internal emission angle, dipole location, layer thicknesses and refractive indices etc. The required material parameters consist of the refractive index dispersion and the thickness of the individual layers as well as the emission spectrum and zone of the emitting layer. The dipole emission model has proven to be a very reliable method for accurately calculating the outcoupled emission spectra of OLEDs, see for instance Refs. [2-3]. It therefore became a crucial tool for device design and optimisation. For instance, the concept of dielectric capping layers for outcoupling improvement or the exploitation of weak cavity effects for colour tuning are of high practical interest. In addition, the comparison of simulation with experimental results allows the extraction of physically meaningful information such as the emission zone or dipole orientation in OLEDs. For advanced analysis ETFOS allows to optimize devices with regards to figure-of-merits (FOMs) that can be defined based on multiple target quantities. The optimization can be carried out with multiple variables.

## 2.3. Validation with Experiments

A quantitative understanding of OLEDs requires reproducible device fabrication that provides extensive and reliable

experimental data for the extraction of material parameters and subsequently for the validation of the models at hand. Combinatorial small molecule OLED fabrication has proven very valuable in this respect [7]. Recently, a combinatorial device fabrication concept has been implemented also for polymer LEDs [8]. In order to demonstrate the accuracy of the optical simulation results we fabricated a series of semitransparent polymer LEDs and studied the outcoupled emission spectra both from top and bottom sides.

The investigated device structure is Al(15 nm)/PEDOT(60 nm)/76% PVK 19% PBD 5% CGR-7160RE (x nm) /Ba(1 nm)/Al (15 nm) and illustrated in Figure 4. This device structure was chosen for validation purposes and not for any practical purpose. Polyvinylcarbazole (PVK) serves as polymeric host material, PBD as the electron-transporting moiety and CGR-7160RE is a red phosphorescent dopant synthesized by Ciba Specialty Chemicals Inc.. Eight distinct PLED devices whose emissive layer thickness is varied were investigated.

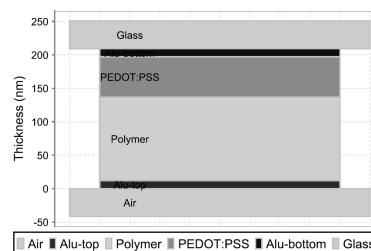


**Figure 4** Illustration of device structure used for the analysis of angular emission through bottom and top sides.

By using thin semitransparent metallic electrodes we are able to analyze both bottom and top emission spectra in this type of OLED. This is useful for checking the simulation results and, in particular, collecting a consistent data set that allows us to extract the single parameter not known beforehand, i.e. the location of the emission zone. In polymeric LEDs the location of the emission zone is frequently not well known. Chances are, that the emission zone is distributed over some region in the device since multiple layers with confining interfaces are not present. The emission zone is a measure of the charge injection and transport balance between electrons and holes.

The experimental data necessary for our analysis comprises the photoluminescence (PL) spectrum of the emitting layer, n&k data and electroluminescence (EL) spectra. In order to derive an accurate device model for the PLED device at hand, we proceed as follows:

1. Model the passive optics (transmittance or reflectance spectra) to determine the thicknesses
2. Model the perpendicular (normalized) emission spectra to find the emission zone
3. Check the consistency with the radiance vs thickness plot
4. Check the consistency with the angular emission characteristics

### 2.3.1. Passive Optics: Transmittance Spectra

In this case of a semitransparent device structure, we choose to use transmittance measurements to model the passive optics. In

the first step we set the refractive index parameters of the individual layer materials and the nominal layer thicknesses in the ETFOS model. Since a series of 8 individual polymer LEDs was fabricated, which differ only in the thickness of the emissive polymer layer, we extracted the polymer thickness from a comparison of the measured and simulated transmittance spectra, see Figure 5.

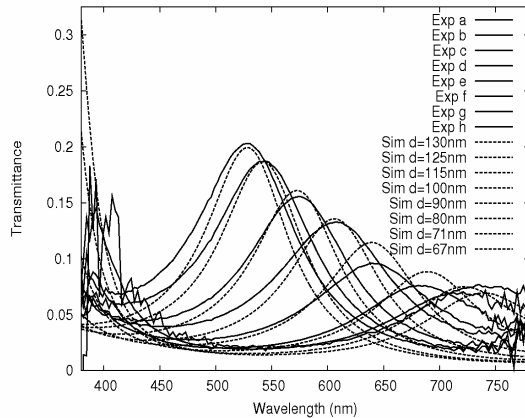


**Figure 5** Comparison of measured and simulated transmittance data for semitransparent polymer LEDs.

The thickness variation was achieved simply by an increase of the polymer spinning speed. From the agreement we conclude that the refractive index parameters used are accurate enough. With this comparison we were able to extract the 8 polymer thicknesses (from 130nm to 67nm) of the polymer LEDs (*a* through *h*).

### 2.3.2. Perpendicular Emission Spectra

We now proceed to extract the location of the emission zone, which in general is not known beforehand if new materials or device structures are investigated. For this step we use the normalized spectra of bottom emission and check 2 crude assumptions: relative dipole emitter location  $r=0$  and 1.  $r=1$  corresponds to the polymer interface with the PEDOT:PSS layer and  $r=0$  corresponds to the interface with the Ba/Al cathode. The comparison is shown in Figure 6, with experimental data plotted with points and corresponding simulated data plotted with lines.

As expected, a redshift in the simulated emission spectra is observed regardless. The peak emission wavelength moves from below 600 nm to above 650 nm in the thickness range from 67 nm to 130 nm. However the strong red shoulder in the emission spectrum is only observed in case of  $r=1$ , i.e. if the dipoles are located at the interface with the PEDOT:PSS layer. Note that a hole transporting moiety was omitted in the polymer blend which may explain why the recombination is highest at the PEDOT:PSS interface.

We have now fixed all simulation parameters and can proceed with investigating how well the simulation predicts outcoupled radiance as well as the angular emission characteristics in both bottom and top emission.

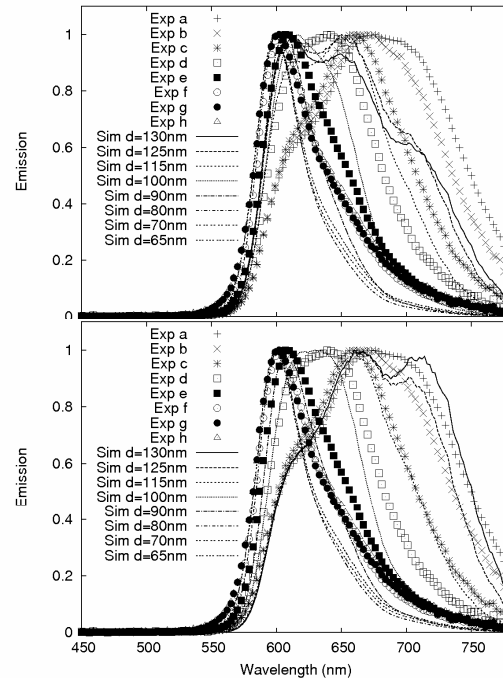


**Figure 6** Comparison of normalized emission spectra assuming dipole location at the polymer/cathode interface (upper panel) and at the PEDOT:PSS/Polymer interface (lower panel).

### 2.3.3. Consistency with radiance vs thickness data

Note that all measurements were taken at the same current density. We thus assume that the electric field distribution inside the polymer layer is comparable in all measurements and thus the current balance should be constant, too. Therefore the most reasonable cause for variations in the measured outcoupling intensities is the occurrence of interference effects. For a first consistency check we now look at the radiance coupled out through the bottom of the PLED, see Figure 7. The simulated radiance peaks at a polymer layer thickness of around 90 nm and roughly agrees with the experiment.

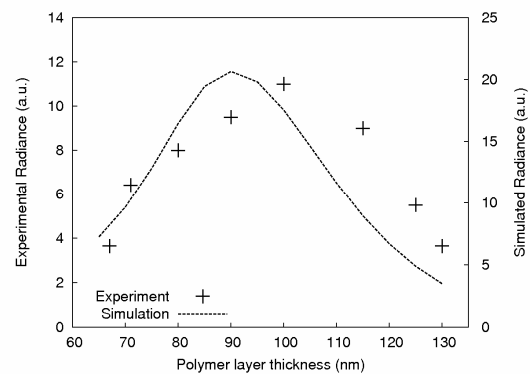


**Figure 7** Comparison of measured and simulated radiance in bottom emission configuration.

### 2.3.4. Consistency with angular emission characteristics

Lastly, we check the angular emission spectra measured both in the bottom and top emission configuration. It is interesting to check the intensity ratio between bottom and top emission, which turns out to be a quantity that is sensitive to the dipole location assumption. However, since we fixed the simulation parameters in steps 1 and 2 we now just check some resulting angular characteristics for consistency. For example we take the two devices *c* and *f* that have polymer layer thickness of 115 nm and 80 nm, respectively, and investigate the angular dependence of the outcoupled radiance.

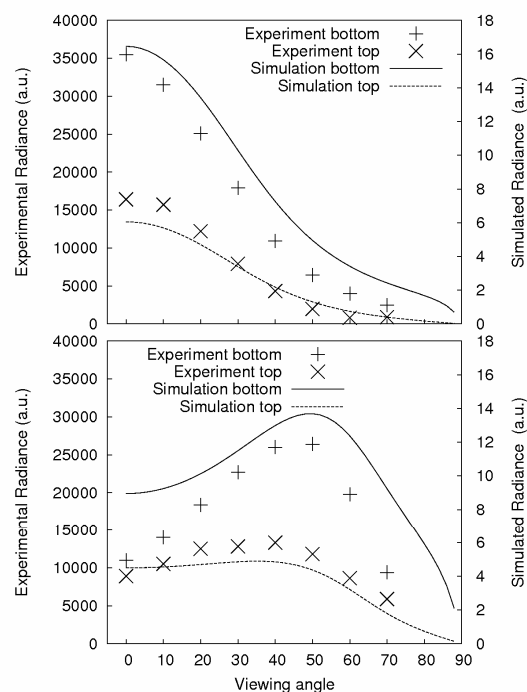


**Figure 8 Comparison of angular outcoupling characteristics in bottom and top emission configuration for an 80 nm (upper panel) and 115 nm (lower panel) thick polymer LED.**

The comparison is shown in Figure 8. It is notable that the 115 nm thick PLED (lower panel in Figure 8) exhibits the maximum radiance at non-zero viewing angle, i.e. at around 50 degrees (in both bottom and top emission). Such a behaviour is generally observed if the optical device thickness is too thick with respect to the peak emission wavelength of the emitting material.

The 80 nm thick PLED (upper panel in Figure 8) shows monotonically decaying radiance with increasing viewing angle and a maximum radiance that exceeds the values observed in the case of the 115 nm thick PLED. The characteristic shape of the angular radiance is again well reproduced with the simulation. In addition it is notable that the ratio of bottom and top emission is well reproduced by the simulation. A last remark refers to the light coupled out through the thick glass substrate. In this case the ETFOS software considers incoherent multiple internal reflections in the substrate and refraction at the substrate/air interface. This is applied in the bottom-emission simulations of Figure 8 and thus is critical for accurate simulation results. The achieved agreements

demonstrate the feasibility of this simulation approach and show a typical application scenario.

For a more detailed analysis, it is recommended to also analyze the s- and p-polarized contributions and refine the dipole location assumption, for instance by setting an exponentially decaying distribution.

### 2.3.5. Fit method for the estimation of the dipole distribution

Finally, we report on further analysis of the emission zone based on a fitting approach [6]. The measured electroluminescence spectra are considered as a linear combination of outcoupled spectra originating from different dipole positions in the emitting polymer layer. With the polymer layer thicknesses taken from the transmittance analysis (Figure 5) we may directly perform such a fit with the electroluminescence spectra in forward direction (see the experimental data in Figure 6). The result of this analysis is shown in Figure 9.

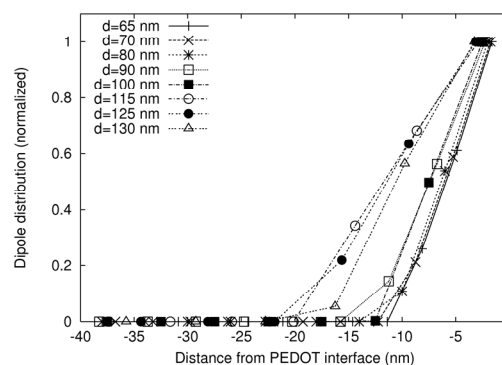


**Figure 9 Dipole distribution fit result for the eight devices discussed above.**

We note that the fits emphasize predominant emission from the anode side of the emissive layer, regardless of the polymer blend layer thickness (ranging from 65 to 130 nm). This result is consistent with the previous estimate of the dipole location at the interface with the PEDOT:PSS layer (see 2.3.2). From Figure 9 we infer a width of the emission zone on the order of 20 nm which is a typical value for the exciton diffusion length. This fit approach is valuable in the analysis of the influences that the injection and current balance, doping, aging or thickness variation has on the emission zone. Moreover it can be employed for parameter extraction. Emission zone fitting can also be performed for validating charge transport model results.

## 3. Conclusion

Our investigations emphasize the importance of thin film effects such as optical interference and electronic confinement. Efficient optoelectronics simulation tools for a careful design of complex multi-layer device structures are presented. These simulator tools can be employed in device research and development dealing with optimization, parameter extraction and fitting. An optical analysis of semitransparent polymer LEDs using angular emission characteristics of a set of OLEDs of varying thickness is carried out. The results demonstrate that the calculated outcoupled emission spectra are accurate for both bottom emission through an incoherent glass substrate as well as top emission through a thin

metal electrode. The optical simulator has a reliable and predictive character and is thus ideally suited to characterize and optimize OLED structures for display and lighting applications. The optical device simulator is extended by electronic device models which have a descriptive and instructive character.

Financial support from the Swiss Federal Commission for Technology and Innovation (CTI) for Project No. 7963.1 is gratefully appreciated.

#### 4. References

- [1] B. Ruhstaller, S.A. Carter, S. Barth, H. Riel, W. Riess, J.C. Scott. Transient and steady-state behavior of space charges in multilayer organic light-emitting diodes. *J. Appl. Phys.* **89**, 4575-86, (2001)
- [2] B. Ruhstaller, T.A. Beierlein, H. Riel, S. Karg, J.C. Scott, W. Riess. Simulating electronic and optical processes in multilayer organic light-emitting devices. *IEEE Journal on Selected Topics in Quantum Electronics, Optoelectronic Device Simulation*, **9** 3, 723-732, (2003)
- [3] H. Riel, S. Karg, T. Beierlein, W. Riess, and K. Neyts. Tuning the emission characteristics of top-emitting organic light-emitting devices by means of a dielectric capping layer: An experimental and theoretical study, *J. Appl. Phys.* **94**, 5290-96, (2003)
- [4] J.M. Leger, S.A. Carter, B. Ruhstaller, H.-G. Nothofer, U. Scherf, H. Tillman, H.H. Hörhold. Thickness-dependent changes in the optical properties of PPV- and PF-based polymer light emitting diodes. *Phys. Rev. B* **68**, 054209 (2003)
- [5] J.M. Leger, S.A. Carter, B. Ruhstaller. Recombination profiles in poly[2-methoxy-5-2-ethylhexyloxy-1,4-phenylenevinylene] light-emitting electrochemical cells. *J. Appl. Phys.* **98** 124907, (2005)
- [6] ETFOS Emissive Thin Film Optics Simulator, commercialized by FLUXiM, see [www.fluxim.com](http://www.fluxim.com) for more details.
- [7] T. A. Beierlein, B. Ruhstaller, D.J. Gundlach, H. Riel, S. Karg, C. Rost, W. Riess. Investigation of internal processes in organic light-emitting devices using thin sensing layers. *Synth. Met.* **138**, 213-21, (2003)
- [8] M. Kiy, R. Kern, T.A. Beierlein, C. Winnewisser. Systematic studies of polymer LEDs based on a combinatorial approach. *Proceedings of SPIE* **6333**, ISBN: 0-8194-6412-0, (2006)